Sains Malaysiana 53(8)(2024): 1937-1952
http://doi.org/10.17576/jsm-2024-5308-17

Microwave vs. Reflux Synthesis of Bis-Thiourea Derivative: Yield Optimization, Crystallographic Understanding and Optical Sensing Potential

(Sintesis Gelombang Mikro lawan Refluks Terbitan Bis-Tiourea: Pengoptimuman Hasil, Pemahaman Kristalografi dan Potensi Penderiaan Optik)

HASANAIN SALAH NAEEM[1,2], ISRAA JABER[2], SUHAILA SAPARI[1], NURUL HIDAYAH ABDUL RAZAK[3], FAZIRA ILYANA ABDUL RAZAK[3], BILAL MAJID RUDAINI[5], ASMAA. SOHEIL. NAJM[4] & SITI AISHAH HASBULLAH[1,*]

[1]*Department of Chemical Sciences, Faculty of Science and Technology, Universiti Kebangsaan Malaysia, 43600 UKM Bangi, Selangor, Malaysia*
[2]*Faculty of Pharmacy, University of Al Muthanna, Samawah 66001, Iraq*
[3]*Department of Chemistry, Faculty of Science, Universiti Teknologi Malaysia, 81310 Johor Bahru, Johor, Malaysia*
[4]*Department of Electrical, Electronics and System, FKAB, Universiti Kebangsaan Malaysia, 43600 UKM Bangi, Selangor, Malaysia*
[5]*Department of Pharmacy, Al-Maarif University College, Al Anbar,31001, Iraq*

Received: 4 December 2023/Accepted: 13 June 2024

ABSTRACT

A new bis-thiourea (BT) derivative was successfully synthesized using both conventional reflux and microwave irradiation methods. The microwave irradiation reaction yielded a greater percentage yield of 73%, while the reflux heating yielded only 44%. The microwave irradiation procedure takes a minimum of 10 min to complete, in contrast to the reflux heating method, which takes 24 h. The compound was characterised using a variety of spectroscopic techniques, including UV-Vis, FTIR, nuclear magnetic resonance (^{1}H-NMR and ^{13}C-NMR), and single crystal X-ray crystallography (XRC). It shows that BT has a high ability to form hydrogen bonds of both intermolecular and intramolecular types, as demonstrated by X-ray crystallography and DFT calculations. In addition, this research provides insights into the possible uses of BT in coordination chemistry involving metal ions, such as a copper ions. Through the use of density-functional theory (DFT) and UV-Vis investigations, it is envisaged that the BT compound has a strong tendency to form stable copper ion complexes. This is supported by the optimal energy value E(UB3LYP) observed for the Cu(II) complex.

Keywords: Bis-thiourea derivative; DFT optimization; microwave reaction; single crystal

ABSTRAK

Dalam penyelidikan ini, sebatian bis-tiourea, BT telah berjaya disintesis menggunakan kaedah konvensional (refluks) dan kaedah penyinaran mikrogelombang. Kaedah penyinaran mikrogelombang memberikan peratusan hasil yang tinggi iaitu 73%, manakala kaedah refluks memberikan hanya 44%. Kaedah penyinaran mikrogelombang memerlukan masa hanya 10 minit untuk selesai berbanding dengan kaedah refluks memerlukan masa sehingga 24 jam. Pencirian struktur sebatian dijalankan menggunakan pelbagai kaedah spektroskopi iaitu spektroskopi ultra lembayung - boleh nampak (ULBN), spektroskopi Fourier transformasi inframerah (FTIR), spektroskopi resonans magnetik nukleus ^{1}H dan ^{13}C (^{1}H-RMN dan ^{13}C-RMN) dan kristalografi sinar-X hablur tunggal (X-Ray). Berdasarkan daripada kajian X-ray dan kajian teori fungsi ketumpatan (DFT), sebatian BT mempunyai keupayaan yang tinggi membentuk ikatan hidrogen secara intramolekul dan intermolekul. Lebih-lebih lagi, kajian ini memberikan penggunaan sebatian BT dalam kimia pengikatan melibatkan ion logam seperti ion kuprum. Melalui kajian fungsi ketumpatan (DFT) dan pemerhatian ULBN, sebatian BT berupaya membentuk kompleks ion kuprum yang stabil. Ini disokong oleh oleh pemerhatian ke atas kompleks Cu(II) melalui nilai tenaga optimum E(UB3LYP).

Kata kunci: Hablur tunggal; pengoptimuman DFT; terbitan bis-tiourea; tindak balas sinaran mikrogelombang

INTRODUCTION

Bis-thiourea derivatives can be described as symmetrical arrangements of bis-thiourea moieties, wherein distinct substituents are present on each side, and a linker is employed to connect the thiourea groups (Al-Harbi, El-Sharief & Abbas 2019; Fakhar, Yamin & Hasbullah 2017). Bis-thiourea derivatives exhibit a diverse array of applications spanning various domains, including catalytic processes, pharmaceutical interventions, biological interventions, and industrial operations. Thiourea, a compound of significant relevance in various industrial applications, exhibits notable properties as a rubber accelerator, corrosion inhibitor, electroplating additive, and precious metal extractor. Thiourea derivatives exhibit remarkable catalytic properties when coordinated with either a nitrogen or oxygen moiety. In recent years, there has been a notable shift in scientific interest toward the exploration of intermolecular forces, particularly in the context of harnessing hydrogen-binding molecules for novel applications in drug development and catalytic design (Jorgetto et al. 2015; Lu et al. 2015; Reisman, Doyle & Jacobsen 2008). Bis-thiourea has been selected as a pivotal molecular entity in numerous investigations for the purpose of generating its derivatives. Furthermore, this compound serves as a catalyst in order to optimise efficiency through its ability to function as a metal detector. The activities exhibited by thiourea derivatives stem from their remarkable capacity to engage in hydrogen bonding interactions, as well as their inherent propensity to possess a surplus of unshared electron pairs within their constituent atoms, namely nitrogen, sulphur, and oxygen. These surplus electron pairs, often referred to as lone pairs, enable thiourea derivatives to engage in π-electron interactions, thereby facilitating their ability to form stable bonds with other elements. The inclusion of π-conjugated systems within thiourea derivatives, commonly referred to as the 'donor-spacer-acceptor' motif, has led to a notable enhancement in electron delocalization within molecular structures, thereby facilitating the presence of multiple donor sites. The phenomenon of metal-ligand binding refers to the intricate interaction between a metal atom or ion and a ligand molecule (Fakhar, Yamin & Hasbullah 2016; Ngah et al. 2017; Saad 2014).

The use of microwave radiation in chemical reactions in microwave chemistry is related to chemical analysis and chemical synthetic processes (Luo et al. 2004; Robinson et al. 2010). However, for use in the synthesis, the frequency of 2.45 GHz has the correct penetration depth for laboratory reactions (Dudley & Stiegman 2015). In a variety of chemical reactions, microwave irradiation outperforms conventional heating methods. The main advantages of microwave-assisted methods are increased reaction rates, which reduce reaction times such as from hours to minutes, increased product yields, and efficient energy conversions (Sapari et al. 2021).

Various sources contribute to the introduction of heavy metal ions into the water and environment, including industrial wastes, batteries, fertilisers, pesticides, petrochemicals, pharmaceuticals, and paper and pulp industries (Baby, Saifullah & Hussein 2019). Copper is essential for maintaining the fluidity of membranes in living cells. Similar to a chemist, it is important to note that copper ions are a significant pollutant in water. These ions can have detrimental effects on the human liver, leading to severe haemolysis and anaemia (Liu et al. 2020). Thiourea derivatives have found wide applications in various fields, particularly in the development of sensors that can detect copper ions (Hosseinjani-Pirdehi et al. 2020). These derivatives are known for their ability to form strong bonds with copper ions through sulphur atoms, even under normal conditions. Because of their unique properties, sulphur atoms can readily form bonds with various metal ions (Bai, Li & Ye 2016), especially copper ions (Maity & Govindaraju 2011).

In this study, the synthesis of bis- thiourea derivative (BT) was synthesised using microwave irradiation and conventional reflux methods. Furthermore, this study compares the percentage yield and reaction time, as well as the mechanism of both approaches. The obtained structure was optimized using the basic set of DFT/RB3-LYP/6-31G/d,p and compared with X-ray crystallographic data. Finally, the optimization geometry of the bis-thiourea derivative with copper metal was carried out. This was subsequently followed by a UV-Vis spectroscopic binding investigation of the bis-thiourea BT and Cu(II) ion.

EXPERIMENTAL

MATERIALS AND INSTRUMENTAL METHODS

Ammonium thiocyanate (≥ 99.5) (Fisher scientific), 3-Methoxybenzyl chloride (99%) (Sigma Aldrich), 2,6-Diaminopyridine (98%) (ACROC), Acetone (> 99.5) (Schmidt), copper(II) acetate monohydrate (Systerm) and Dimethyl sulfoxide-d (DMSO-d6) (≥ 99.8) (Sigma Aldrich) were used as received.

The microwave reactor (Anton Paar Monowave 450) is an irradiation method for the synthesis the bis-thiourea derivative compound. Furthermore, the 400 MHz of Bruker Avance III HD 400 Nuclear Magnetic Resonance Spectroscopy (NMR), Fourier-Transform Infrared Spectroscopy (FT-IR), Ultraviolet- visible Spectroscopy (UV-Vis), and single crystal X-ray crystallography were used for structural characterization.

GENERAL PROCEDURE FOR THE SYNTHESIS OF BIS-THIOUREA DERIVATIVE COMPOUND (BT)

Bis-thiourea BT was synthesized as described by Nurul Hidayah et al. (2020) (Figure 1). The solution of ammonium thiocyanate (0.152 g, 0.002 mol) in dried acetone (5

mL) was prepared and added dropwise to the solution of 3-methoxybenzoyl chloride (0.341 g, 0.002 mol) in dried acetone (5 mL) and stirred at a room temperature. The precipitate formed by the reaction was filtered off. A solution of 2,6-diaminopyridine (0.109 g, 0.001 mol) in dried acetone (5 mL) was added to the filtrate and then refluxed at 80 ºC for 24 h (in conventional synthesis) and 2 h, 1 h, 10 min (in microwave synthesis). The obtained mixture was filtered into a beaker filled with enough ice to produce a pale-yellow precipitate. m.p: 216-217 °C. (KBr/cm^{-1}) 3317 υ(N-H), 1024 υ(C=S), 1643 υ(C=O), 1513 υ(C=N),1326 υ(C-N), 1443 υ(Ar-C), 3068 υ(sp^2-C-H), 2837 υ(sp^3-C-H), 1138 υ(C-O). δ^1H (500 MHz, $DMSO_{d6}$) 13.25 (2H, *s*, N-H_{amide}), 11.83 (2H, *s*, N-$H_{thioamide}$), 7.23 (2H, *d*, *J* = 7 Hz, Ar-H_3), 8.03 (1H, *t*, *J* = 8.11 Hz, Ar-H_4), 8.6 (2H, *s*, Ar-H_{10}), 7.46 (2H, *t*, *J* = 7.93 Hz, Ar-H_{12}), 7.57 (4H, *m*, Ar-$H_{13,14}$), 3.85 (6H, *s*, -OCH_3). δ^{13}C (125 MHz, CDCl3) 178.5, 168.6, 150.3, 113.4, 140.6, 133.8, 130.1, 159.5, 113.8, 120, 121.5, 55.9. UV-Vis: 277 nm (ε = 20433.3 M^{-1} cm^{-1}) and 314 nm (ε = 17866.6 M^{-1} cm^{-1}).

COMPUTATIONAL STUDIES (DENSITY FUNCTIONAL THEORY DFT)

The density-functional theory (DFT) is a successful calculation theory for atoms, molecules and solids electronic structure. Its aim to understand the material characteristics of the fundamental laws of quantum mechanics quantitatively. Geometry optimizations were performed using Becker's three parameterized Lee-Yang-Par (B3LYP) exchange functional method with 6-31G(d,p) basis set (Gemili et al. 2018). For the complexation of a bis- thiourea with Cu(II), the calculations were performed using Gaussian 16 and visualized by Gaussview 9 software at Center of Information and Communication Technology, Universiti Teknologi Malaysia. The geometry optimisations were conducted by DFT using Becke's three-parameter exchange functional, the Lee-Yang-Parr correlation functional (B3LYP) method. These functions were applied with the hybrid GEN method with 6–31G(d, p)++/ to all of the atoms of BT ligand and basis set of Los Alamos National Laboratory 2 Double-Zeta (LANL2DZ) was used on the transition metal of copper (Wazzan 2015). Combined with density functional approaches, these basis sets have been extensively utilized in the study of transition metal systems (Han et al. 2009). For this study, we employed the '6–31G(d,p) + LANL2DZ' mixed basis set, which incorporates the Los Alamos Effective Core Potential for the transition metal (copper ion Cu^{2+}) (Wazzan 2015). A computational method called LANL2DZ was employed to simulate the behaviour of metal atoms. In recent years, mixing basis sets of this type have gained popularity in the study of transition metal systems and computational chemistry studies. These basis sets, along with density functional methods, have been widely used and have been the focus of research (Yang, Weaver & Merz Jr. 2009).

INVESTIGATION OF THE BINDING OFBT COMPOUND WITH CU(II)

The energy region for the UV-vis section of the electromagnetic spectrum spans from 1.5-6.2 eV, corresponding to a wavelength range of 800-200 nm. A bis-thiourea derivative compound (0.132 mg, 3×10^{-5} M) was mixed with 10 mL of distilled water solvent and shaken until fully dissolved. It was then bound with copper metal ions. A solution of copper ions was prepared with a concentration of 1×10^{-5} M. Finally, combining the solutions of BT and Cu(II) in a 1:1 ratio.

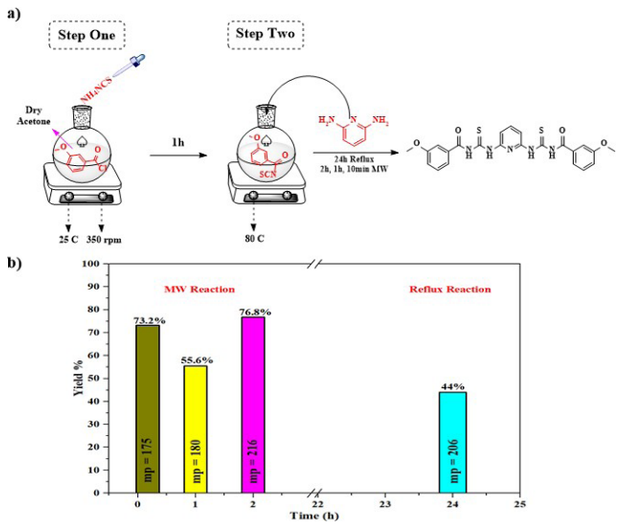

FIGURE 1. Bis-thiourea (BT) synthesis by using reflux method (a) comparison of time and yield of both method (b)

RESULTS AND DISCUSSION

Several studies have been attempted to synthesize sulfur urea by heating ammonium thiocyanate (Schroeder 1955; Warren 1928). Maddani and Prabhu (2010) have discovered a simple and efficient process for producing di- and tri-substituted thiourea derivatives in aqueous conditions with high yields. In comparison to standard heating methods, MW irradiation has a shorter reaction lifetime and higher yields for products (Bruckmann, Krebs & Bolm 2008). Bis-thiourea compounds are among the main chemicals employed as bi-chelated ligands. Color changes or fluorometric fluorescence changes are produced by complexes generated from bis-thiourea and copper compounds. Furthermore, the C=S and C=O moieties of the acyl thiosemicarbazide group are remarkably similar to Cu(II) (Jin et al. 2014; Lin et al. 2013; Tungsombatvisit et al. 2019).

CHARACTERIZATION

Ultraviolet-visible spectroscopy (UV-Vis)

Figure 2 shows the ultraviolet-visible absorption spectrum of BT compounds. The electronic absorption spectrum of the BT compound has two broad background absorption peaks and was recorded in DMSO (30 mM). The maximum absorption bands of the BT compound are at 277 nm (ε = 20433.3 M^{-1} cm^{-1}) and 314 nm (ε = 17866.6 M^{-1} cm^{-1}) and can be attributed to the transitions of the n→π* electrons resulting from the long pair of which arise from the lone pair of oxygen and sulfur electrons of C=O and C=S (Abosadiya et al. 2015). This transition corresponds to the electronic orbital transition from HOMO to LUMO. The addition of auxochromes methoxy substituent groups in the *m*- position, which increased the electron conjugated bond in the phenyl ring, as well as the presence of NH groups in the spectra, results in a bathochromic shift (Mohd et al. 2011).

At 277 nm, the first transition has a higher molar absorptivity. It is equivalent to π→π* (LUMO) transition. It includes more contributions from both π bonding orbitals HOMO-1 and HOMO-2. The p_z orbital of the sulfur atom forms HOMO-1, and the p_z orbitals of the carbon atoms of the 3-methoxyphenyl and pyridine rings form HOMO-2. The second transition at 314 nm is associated with a wider range of n → π* transitions, where electrons move from non-bonding (n) orbitals to π* antibonding orbitals. These transitions mainly occur due to the unbound electron pairs of atoms that have an abundance of electrons, like oxygen and sulphur.

The molecule S, N, and O are occupied by empty molecular orbitals. Furthermore, the absorption peak at 314 nm indicates that the BT compound is a chromophore in the visible region. The presence of free non-binding electron pairs (n) of electron-rich atoms caused the BT compound absorbs visible light. This region's light has a lower energy and can only excite non- binding electrons.

Fourier-transform infrared spectroscopy (FT-IR)

Figure 3 depicts the FT-IR spectrum of BT, and all functional groups identified in the BT compound were assigned. In the part of the compound, the primary amine N-H and thiocarbonyl C=S have two distinct vibrations (Pingaew et al. 2017). The appearance of the broadband with a single peak at region 3317 cm^{-1} corresponds to the stretch frequency of the secondary (N-H) group, whereas the stretching absorption band value for the (C=S) groups appeared to be 1024 cm^{-1}. Because the S atom has a lower electronegative charge than the O atom, the C=S group is less polar than the C=O group and it is less likely to form intramolecular hydrogen bond bridges (Chacko Yohannan Panickera et al. 2010). The normal value of ν(C=S) stretching vibrations is 1050-1200 cm^{-1} (Abosadiya et al. 2015). The slight decrease in the stretching vibrational frequencies of C=S bonds is due to nitrogen's mesomeric electron releasing effect on the thiocarbonyl group.

Subsequently, IR spectra for this derivative show the presence of three sharp-peaks vibrations at the (C=O), (C=N), and (C-N) groups, with reported values of 1643 cm^{-1}, 1513 cm^{-1}, and 1326 cm^{-1}, respectively (Adam, Fatihah & Ameram 2016). These vibrational frequencies were vibrating in the lower region due to the resonance effect of (C=O amide) when the unpaired electrons on a nitrogen atom conjugated with the carbonyl group, as well as the presence of intramolecular hydrogen bonds between the carbonyl group and the hydrogen atom attached to the thiocarbonyl group (H-N- C=S). While C=C bonds vibrated at 1443.4 $cm^{-1}$and 1423.8 cm^{-1}, sp^2-C-H appeared at 3068.5 cm^{-1}. Two distinct peaks were obtained for the methoxy group at 2837.4, 1483.4, and 1138.7 cm^{-1}, which correspond to stretching sp^3-C-H, -CH_3 (methyl group), and C-O, respectively.

Nuclear magnetic resonance spectroscopy analysis (NMR)

Figure 4 shows the ^{1}H-NMR spectrum of BT. Two distinct peaks were observed at δ 11.83 and δ 13.25 ppm, which were attributed to the presence of N-H protons in two different environments. The nearby carbonyl and thionyl groups have a strong deshielding effect and the amide proton is less shielded than the thioamide proton (Kole & Kumar 2018; Sapari et al. 2021). Due to geometrical constraints, intramolecular hydrogen bonds are formed between the oxygen of the carbonyl groups and the hydrogen atom in the S=C-NH-pyridine part (C=O---H-N) and formation of the six-membered ring (Dhanishta et al. 2018). Furthermore, the DMSO-d_6 forms an intermolecular exchange H-bond

between N-H and C=O of DMSO-d_6, causing the N-H protons to shift downfield (Charisiadis et al. 2014).

The peak for $H^{3,3'}$ and H^4 pyridine ring protons were appeared at 7.23 ppm and 8.03 ppm, respectively. As expected, the presence of oxygen has a de-shielding effect on methoxy protons and appears at 3.85 ppm. Finally, the appearance of a single broad peak at 8.6 ppm was attributed to $H^{10,10'}$ due to the shielding effect of the methoxy group removed by electron-withdrawing groups of carbonyl groups. While the $H^{14,14'}$ and $H^{12,12'}$ appeared at 7.57 ppm and 7.46 ppm, respectively, due to the inductive removal of carbonyl electrons, $H^{12,12'}$, and $H^{14,14'}$ have a de-shielding effect.

Figure 5 shown the ^{13}C-NMR spectrum for BT compound. The ^{13}C chemical shifts at 178.5 ppm and 168.6 ppm were attributed to thionyl and carbonyl groups, respectively (Kamalulazmy et al. 2016). C^{11}, which is attached to the methoxy group, has a peak at 159.5 ppm. C^2, C^4, and $C^{9,9'}$ were assigned three different peak positions at 150.3 ppm, 140.6 ppm, and 133.8 ppm, respectively. The ability of function groups associated with aromatic rings to increase and decrease the ring's electron density. Deshielding was greater for C^2 and C^4 than for C^9 due to the ability of the N atom in the pyridine ring to remove electronic density from ortho and para positions. C^{10} was observed at 130.1 ppm due to C^{10} work as a short bridge to transfer electron density from the methoxy group to the carbonyl group, whereas the electron density is concentrated at C^{12}, which was observed at 113.8 ppm and appears as an overlapping peak with the C^3 peak at 113.4 ppm. The methoxy group, on the other hand, caused C^{14} to appear at 121.5 ppm and had a minor effect on C^{13} meta position at 120 ppm.

THE CHEMISTRY AND MECHANISM OF THE BIS-THIOUREA DERIVATIVE (BT)

Reflux heating method

In a two-step reaction, bis-thiourea BT compound was synthesized with a low yield. In the first step of the reaction, 3-methoxy benzoyl chloride was mixed with ammonium thiocyanate in dried acetone under moderate conditions (room temperature and 350 rpm). 3-methoxy benzoyl chloride is regarded as a good starting material for reactions at normal and high temperatures (Imran Fakhar et al. 2018), as well as at lower temperatures (Mohd et al. 2011). Aryl isothiocyanates (Ar-NCSs) are important synthetic intermediates for gaining access to various compounds containing valuable sulfur. They belong to the organic chalcogen cyanide (Ar-NCS) chemical class, in which the heteroatom (N) is linked to the organic substituent (aryl) by a single bond and the CS group by a different one.

Due to the presence of the electronegative nitrogen atom, the pyridine aromatic ring linker has an electronic deficiency, with positions 2, 4, and 6 on the pyridine ring being the most affected. The reactivity of substituents in these heterocycles is affected by the deficiency, particularly in the more electron deficient sites (Caprio 2008). The amino groups at the 2- and 6-positions of the pyridine ring are electron deficient due to the loss of the electron density to the ring nitrogen *via* resonance and induction, The relative ease of deprotonation at the 2- and 6-amino positions to produce resonance-stabilized anions is a result of this effect. The 2,6-diamine pyridine compound was one of the factors that significantly reduced the yield due to the decrease in the electronic density at these two positions, which resulted in a decrease in the electronic density of the nitrogen atoms in the primary amine groups. The hydrogen in primary amine groups is acidic, and the imine group in aryl isothiocyanates (which are more basic than primary amine groups) attracts proton and forms the conjugated base pyridine-NH-, according to the reaction mechanism in Figure 6 (Arshad et al. 2024). However, amino groups were in contact with a closed delocalization system, both amino groups on the pyridine ring interacted with aryl isothiocyanates parts sequentially rather than simultaneously.

The solvent may influence the reactions and their stability. Due to the small amounts of water that could affect and quench the reaction, dry acetone was used as a solvent for the reaction. Chloride groups are good leaving groups causing the water to easily interact with 3-methoxybenzoyl chloride and form a carboxylic group, and the carbonyl will promote the ability of the chloride group to leave and then quench the reaction. One of the reasons for the decrease in yield (44%) was the solubility of the 2,6-diamine pyridine compound. The pyridine linker compound is more soluble in polar protic solvents and has good solubility in polar aprotic solvents. Due to the presence of the benzoyl chloride group, polar protic solvents could not be used in our reaction, and the reaction would come to a halt. As a result, polar aprotic solvents (dry acetone) were used as the solvent system.

Microwave irradiation method (MW)

In microwave vials, microwave experiments with efficient mechanical stirring were carried out (avoiding all non-homogeneity temperature problems). Experiments were carried out in triplicate to achieve the best results. Under the same conditions, the yield of the products is 77%, 56%, and 73% for 2 h, 1 h, and 10 min, respectively. In all cases, reactions occurred at similar temperatures with significantly higher yields when heated conventionally, demonstrating that the effect of MW is clearly not thermal.

The dipole rotation of the polar solvent molecules is primarily responsible for the microwave solution (dry acetone). According to the dipolar polarization mechanism, the rotation of acetone molecules resulted in the rotation of the starting materials in the solution and an increase in temperature (Jin et al. 2014).

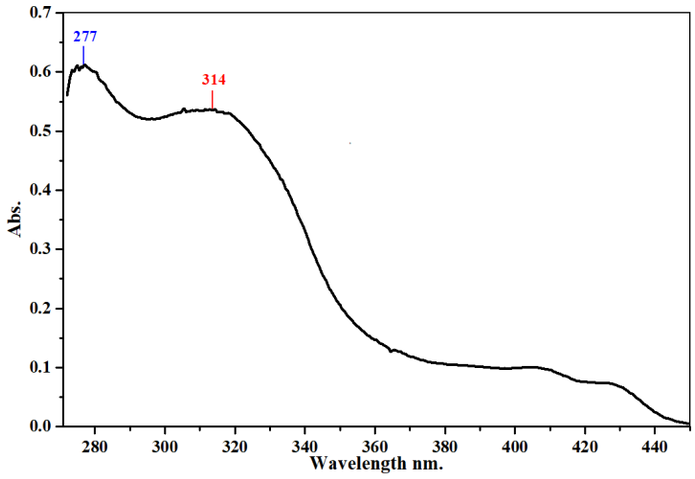

FIGURE 2. UV-Vis spectrum of bis-thiourea derivative compound (BT)

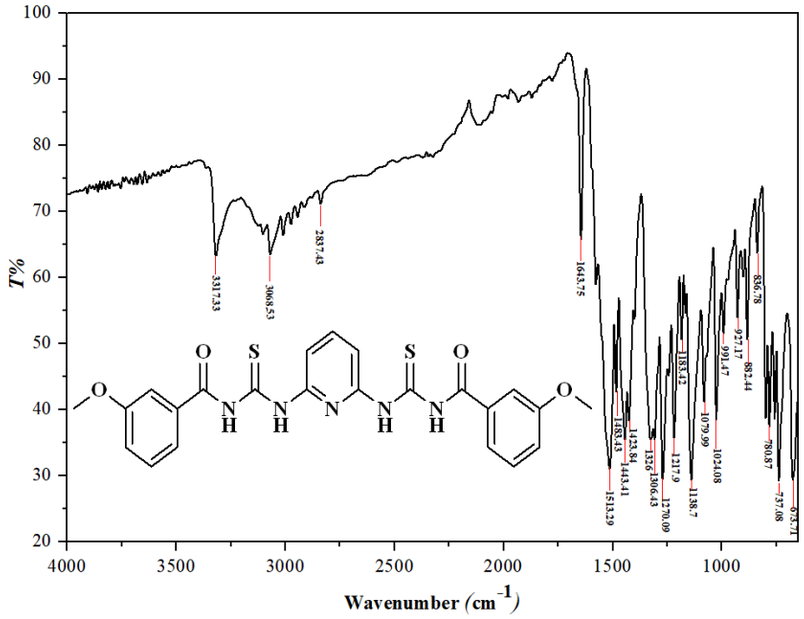

FIGURE 3. FT-IR spectrum of BT compound

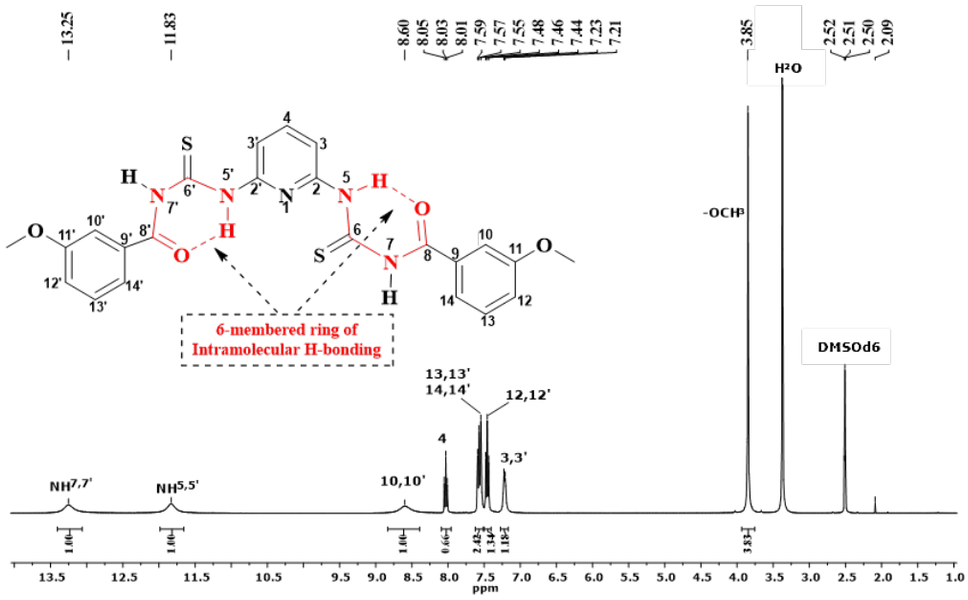

FIGURE 4. ^{1}H-NMR (DMSO.d$_6$ 400 MHz) spectrum of bis-thiourea BT compound

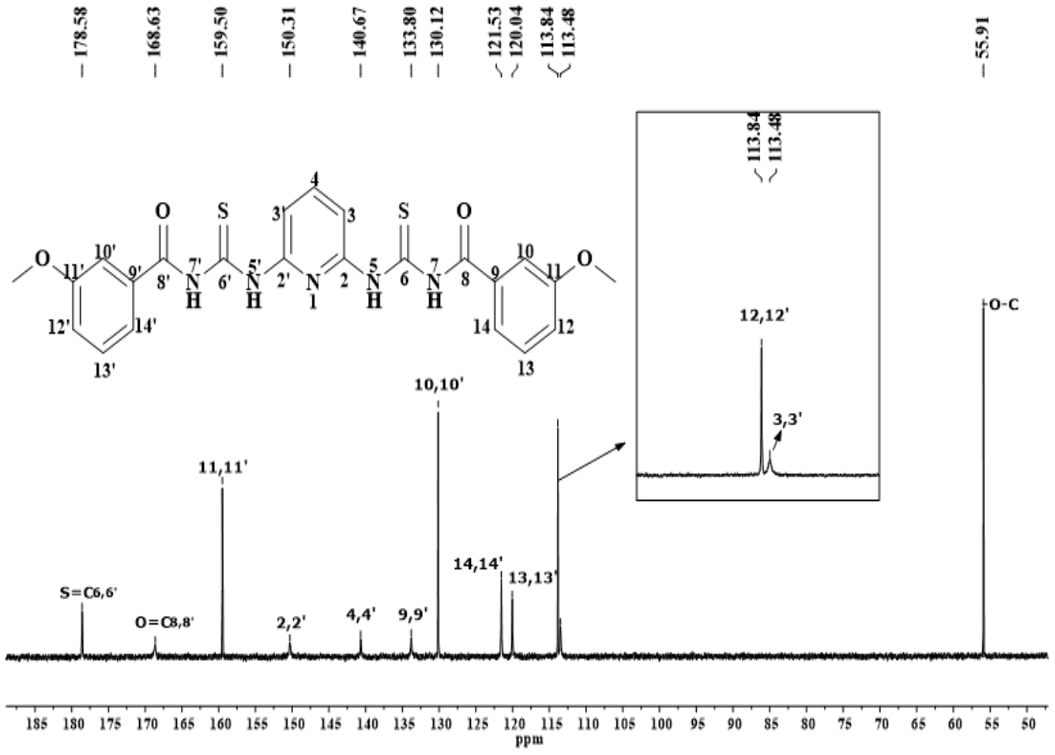

FIGURE 5. ^{13}C-NMR (DMSO.d$_6$ 100 MHz) spectrum of BT compound

Furthermore, the starting materials (diaminopyridine and 3-methoxybenzoyl isothiocanate) are polarized, they are rotated in all directions. The displacement of the charge from its average equilibrium position causes dielectric polarization, where the dielectric material, through which the charged particles cannot freely move, is exposed to an external electrical field. This polarization is classified as follows: i) electronic polarization caused by electron displacement from nuclei, ii) atomic polarization caused by atomic nuclei displacement, iii) dipolar polarization caused by reorientation of molecules with permanent dipoles, and iv) interfacial polarization caused by an accumulation of relatively mobile charges at grain/phase boundaries or surfaces (Klygach et al. 2019; Tang, Radosz & Shen 2008). According to this scientific evidence, the effect of microwave radiation on electrons, atoms, and molecules in a reaction solution can be predicted.

The reaction begins with increased resonance in the pyridine ring and is polarized by an applied electric field of 2,6-diaminopyridine molecules. The electron displacement of the nitrogen nucleus in the pyridine ring, as well as the electron displacement of the heterogeneous aromatic ring and the amine groups in the ortho positions, polarize the large electron displacement to the nitrogen atom. The pyridine nitrogen atom forms a strong hydrogen bond, and *Intramolecular Proton Transfer (IPT)* occurs between the hydrogen of one amino group and the pyridine nitrogen atom (Antony Muthu Prabhu et al. 2010). When 3-methoxy benzoyl isothiocyanate molecules are exposed to microwave radiation, electrical and atomic displacements occur (Antony Muthu Prabhu et al. 2010). The carbonyl group's oxygen atom and the imine group's nitrogen atom will have a higher electron density than the other parts (oxygen will have an electron density from the 3-methoxy benzoyl ring; thionyl nitrogen). Excited molecules (2,6-diaminopyridine and 3-methoxy benzoyl isothiocyanate) approach each other to react by donating the transported proton to the nitrogen imine group while a strong nucleophilic (amine group) attacks the polarized carbon atom in the thionyl group, as shown in Figure 7.

During the same period, differentials will be used to form the second part of BT compound. IPT, which reduces the effect electron-deficiency of the nitrogen atom on the pyridine ring, caused the effect electron-deficiency of the second amino group to be approximately isolated. As a result, the second amino group will be polarized, allowing the excited 3-methoxy benzoyl isothiocyanate molecule to easily react with the second amino group by attacking nitrogen in the proton's imine group while the amino group attacks carbon in the thionyl group.

After ten minutes, the product was crystalline and the increase in collision time within the solution caused the crystalline formation to shatter, and the period of shattering can be predicted. The ten minutes reaction product contained a small amount of aggregations that could be seen with the naked eye. As the reaction time increases (2 h and 1 h), the resulting crystals collide with each other, causing the crystal to break down and the molecules to be bound together by irregular intermolecular hydrogen bonds, forming the aggregations.

COMPARISON OF EXPERIMENTAL AND THEORETICAL STUDIES FOR BT COMPOUND STRUCTURE

Experimental measurements deal with a molecule's solid phase, whereas theoretical calculations deal with a molecule's gas phase (Altaf et al. 2015). As a result, most of the values of bond lengths and angles for a molecule differ little. DFT methods typically deal with a single molecule in the unit cell, whereas single crystal studies deal with both a single molecule and packing molecules in the unit cell (Teixeira et al. 2012). The DFT optimized geometry was compared to the crystal structure, which is compatible approximately with the crystal structure of XRC analysis. Table S1 shows the given crystal state and refinement parameters. Table S2 shows the crystallographic and optimized geometric bond lengths and bond angles of BT compound.

Experimentally, the synthesized BT compound was found to be in a monoclinic crystal system in the single crystal study. The space group and unit cell parameters of BT compound was C2/c, a = 21.1960 (19) Å, b = 11.9137 (10) Å, c = 9.0331 (6) Å, $\alpha = \gamma = 90°$, $\beta = 94.679$ (3) °, V = 2273.5 (3) $Å^3$, Z = 8. The occurrence of distortion in the geometry of nitrogen atoms as a result of the surrounding environment, which makes predicting its geometry on the basis of hybridization difficult (Altaf et al. 2015).

Experimentally, the lengths of the bonds at the N2 atom are N2-C4 (1.338 A^o) and N2-C3 (1.401 A^o), respectively, while the N3 atom has N3-C5 (1.369 A^o) and N3-C4 (1.403 A^o). This is because the oxygen atom has a higher electronegativity than the sulphur atom. The length of the O1-C5 (1.230 A^o) bond, on the other hand, is longer than that of the S1-C4 (1.644 A^o) bond due to electron density delocalization towards the carbonyl group, which is consistent with previous literature (Arshad et al. 2020). The angle of bonds shows the concentration of the electronic density as well as the movement of electrons in the compound's two most important active sites, namely the amide and thio-amide groups. The angle N3-C4-S1 (117.68^o) is smaller than the angle O1- C5-N3 (122.05^o). This means that the N3 atom increases the electron density on the carbonyl group more than on the thionyl group. The angle of N2-C4-S1 (128.87^o), on the other hand, was much larger than the previous angles, indicating that N2 supplies the thionyl group with a large electron density, which then withdraws a large electronic density from the pyridine ring. The electron density of the C5 atom N3-C5-C6 (117.03^o)

was higher than that of the C5 atom N2-C4-N3 (113.45°), as shown in Figure 8.

Except for the C1-C2 (1.377 A°) bond, which has a difference of less than (0.013 A°), the lengths of the pyridine ring bonds were nearly equal (1.388 A°), and this difference may be due to the withdrawal of the electronic density by the thioamide group and the nitrogen atom in the pyrene ring. The C3-N1-C3 (118.6°) angle, on the other hand, was much smaller than the other pyridine ring angles (C1, C2, and C3) because N1 is basic in nature, which means that the alone electron pair and the electron density gained from the resonance phenomenon of aromatic compounds tend to be highly concentrated outside the ring. By comparing the length of the O2-C10 (1.361A°) bond to that of the O2-C12 (1. 419A°), the methoxy group demonstrated its electron-donating properties.

The single molecule's stability and structure are maintained by intramolecular hydrogen bonds, whereas crystal packing in the unit cell is maintained by intermolecular hydrogen bonds (Delgado et al. 2024). The average distance of $[N2\text{-}H2\text{---}O1]_{intra}$ hydro- gen bonding was 2.202 A°, which is slightly greater than the re- ported distance of 2.28 A° (Fakhar, Yamin & Hasbullah 2017). Table 2 summarizes the data relevant to crystal structure determination. It should be noted that the geometry of the prepared bis-thiourea derivative was very close to planar due to the number of intramolecular hydrogen bonds that worked to achieve the highest degree of stability, as shown in Figure 9(a). The single crystal was formed by packing the intermolecular hydrogen bonds $[C7\text{–}H7\text{---}O1]_{inter}$ and $[N3\text{–}H3\text{---}O1]_{inter}$, as shown in Figure 9(b) and 9(c).

The optimum energy value for BT compound -5934041.870507 kJ/mol as determined by DFT structure optimization. Theoretical studies of the BT molecule showed that it belongs to the C1 symmetry point group with dipole moment is 2.437886 D. The calculation method was used B3LYP (restricted) and singlet spin with polarizability (α) equal 345.869000 (a.u.). The comparison of the data obtained from the improved geometry DFT with the experimental data supports the crystal structure of the prepared derivative from the theoretical side. There are bond length matches between atoms that do not participate in the formation of the single crystal (atoms had inter- and intramolecular H-bonds). The majority of the 3-methoxybenzoyl bonds, for example, were equal or close in length. This shows that the ability to withdraw the electronic density occurring inside the molecule (experimental calculations) by the phenomenon of delocalization by the thioamide group as well as the phenomenon of resonance by the nitrogen atom in pyridine differs from theoretical calculations by DFT (Effendhy et al 2024). This means that each molecule (whether prepared or natural) has a unique molecular environment. If the molecule is used in an applied field, its molecular environment controls all of its activities. As a result, when the researcher deals with this molecule in the applied field, the molecule's environment must be taken into account by not exposing it to high energy fields, which leads to its destruction. It can, however, be dealt with by using another molecule or metal that works for this environment.

OPTICAL SENSING PROPERTY OF THE BT COMPOUND WITH CU(II)

We investigated the optimized structure of the BT compound by interacting copper into it, the thionyl groups serving as the active site. The optimum energy value for the complex BT-Cu -6449368.105315 kJ/mol as determined by DFT structure optimization. Theoretical studies of the BT-Cu complex showed that it belongs to the C1 symmetry point group with dipole moment is 0.935585 D. The calculation method was used UB3LYP (Unrestricted) and Doublet spin with BSSE (Basic Set Superposition Error) energy equal -170.850495 kJ/mol. When copper binds to the ligand, it produces a lower-energy compound, which is more stable compound (Alenzi et al. 2024). There were significant differences in the lengths and angles of the ligaments. Thioamides are known to have larger rotational barriers than amides, where the barrier is formed by the amide nitrogen interacting with the adjacent C=O or C=S group (Wiberg et al. 2011). Because of the polarization of the thionyl group by the copper atom, the length of the S1-C4 (1.716 A°) bond has increased significantly. It also lengthened the bonds close to the thionyl group, particularly the pyridine ring, which plays an important role in directing the charge to the thioamide group, as shown in Figure 10.

When copper solution was added, the BT ligand's maximum wavelength was shifted to a bathochromic and the absorbance was lowered. The BT ligand spectra showed two low peaks at 402 and 425 nm (transitions, which were caused by the amide and thioamide groups, respectively (Ajlouni et al. 2012). The peaks of thioamides are lower than those of amides (Jambi et al 2023; Perrone, Monteiro & Castelo-Branco 2015). According to the DFT of the BT- Cu optimization, Cu(II) connected with the BT ligand through thionyl groups, but the bonding occurred by thionyl and carbonyl groups combined according to the UV-Vis spectrum. In general, two molecules of acetate are bound to copper via the 4s and 4px orbitals. When interacting with the ligand, copper 'soft acid' withdraws the electronic density from the thionyl and carbonyl groups 'soft base', forming weak coordination bonds. The rotation of the amine groups (as indicated above, the capacity of the thioamide groups to considerably rotate) modified the geometry of the BT ligand, forming a huge tetra-chelating cavity. Low peaks of the thioamide group and the amide group have totally disappeared from the curve due to hypsochromic shift, which was derived from careful observation of the UV-Vis spectra. Also, the (*) peak has been reduced to a weakness and broad peak. The change in the electrons of the double bonds (aromatic rings), as well as alone electron pairs on

the N, S, and O atoms, is responsible for this shift 337 nm, as shown in Figure 11. Copper has a strong electrostatic attraction, causing the electrical density of aromatic rings and alone electron pairs to shift towards the metal. As a result of coordinating with the copper metal, electrons withdrawing from Cu(II) have reduced the delocalization phenomenon. This also explains why the color of the BT compound solution after addition changed from pale yellow to yellow due to the restriction of the electrons of the thioamide and amide groups, which caused the electron density surrounding these groups to absorb lower wavelengths (higher energies) in order to excite them from HOMO to LUMO

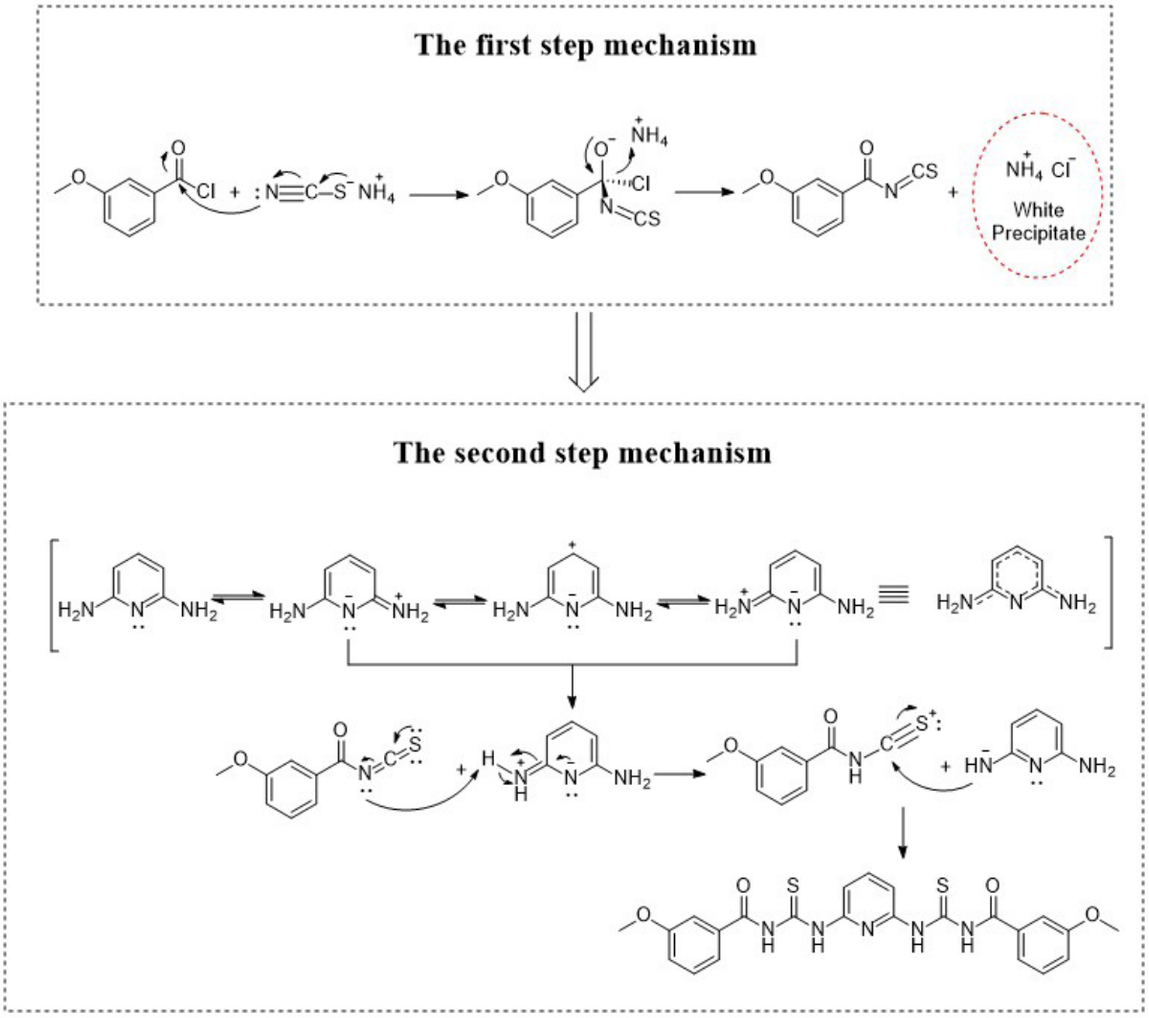

FIGURE 6. The proposed mechanism for the synthesis of BTcompound under reflux condition

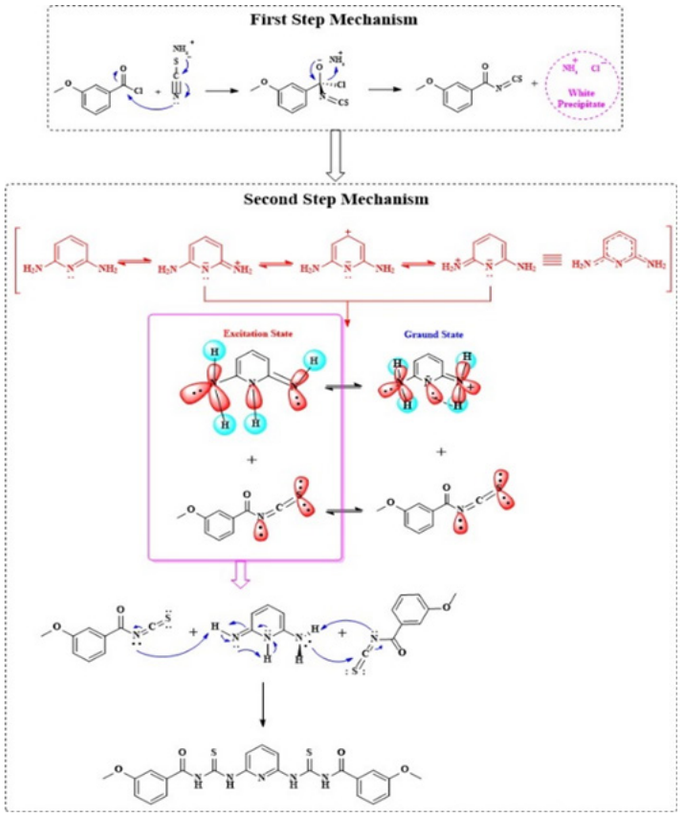

FIGURE 7. The proposed mechanism of the synthesis of BT compound under microwave irradiation method

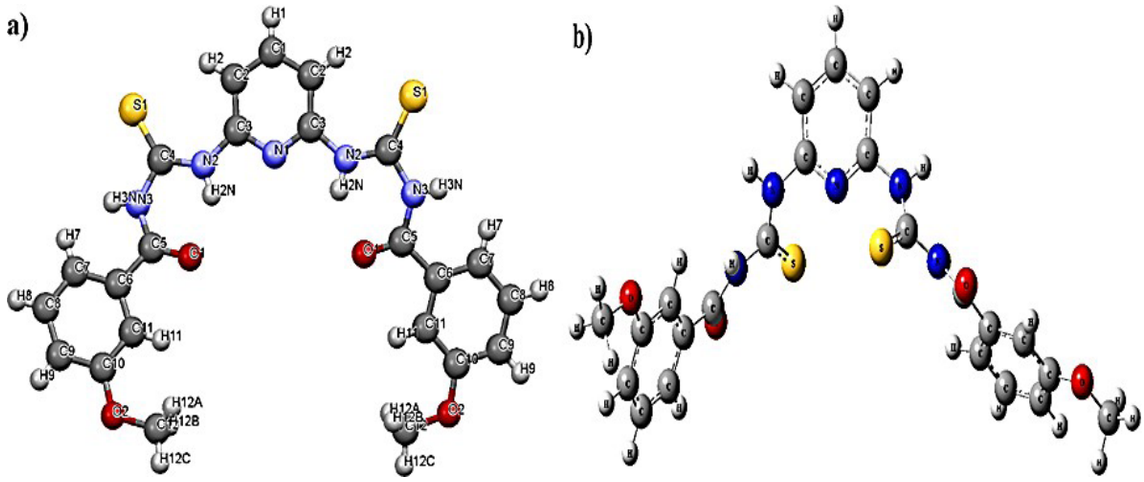

FIGURE 8. The BT compound structure at a) the experimental molecule structure (publication plot), and b) the DFT-optimized molecule geometry

TABLE 2. Inter- and intra-molecular hydrogen bonds for BT [(Å) and (°)]

D–H…A	d(D–H)	d(H…A)	d(D…A)	<(DHA)
$[N2–H2\cdots O1]_{intra}$	0.82	2.202	2.631	139.84
$[C11–H11\cdots O1]_{intra}$	0.93	2.452	2.761	99.36
$[C2–H2\cdots S1]_{intra}$	0.93	2.655	3.277	124.96
$[C7–H7\cdots O1]_{inter}$	0.93	2.719	3.149	109.14
$[N3–H3\cdots O1]_{inter}$	0.82	2.202	2.906	143.61

Symmetry transformations used to generate equivalent atoms: # x,y,z # x,1-y,-1/2+z # x,1-y,1/2+z.
The Symmetry code: (i) −x+1, y, −z+1/2

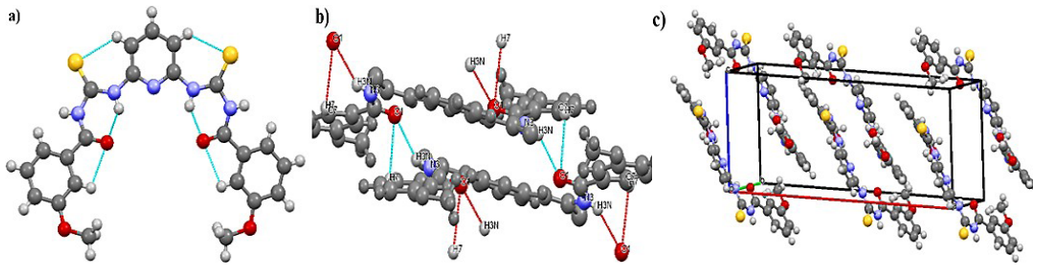

FIGURE 9. Crystal structure (XRC) of the bis-thiourea derivative compound (BT), a) the dashed line indicates the intramolecular hydrogen bond, {b) the intermolecular hydrogen bond, and c) Molecular packing of BT viewed down the a-axis

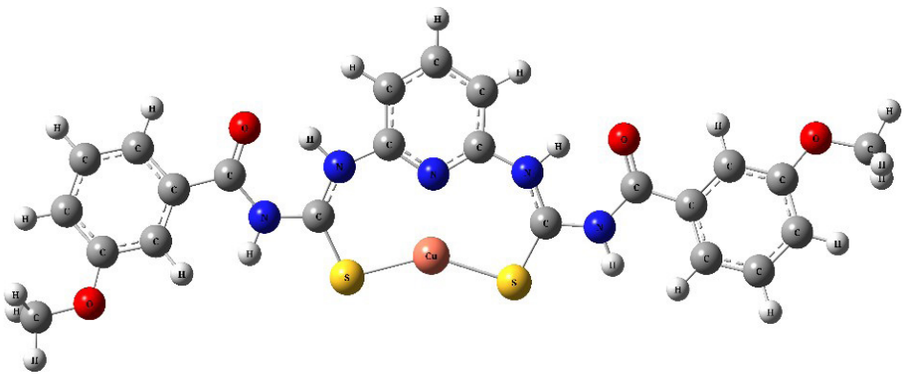

FIGURE 10. The optimized BT-Cu(II) structure by using DFT calculation, UB3LYP/GEN '6–31G(d,p) + LANL2DZ' method

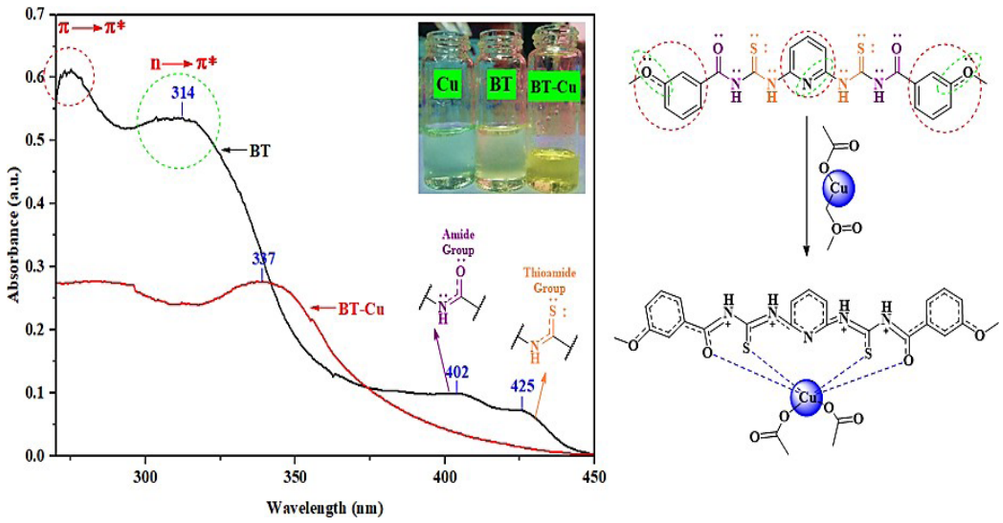

FIGURE 11. UV-Vis spectrum of BT compound binding to Cu(II) and its proposed binding interaction

CONCLUSION

Bis-thiourea (BT) has been synthesized by a reflux reaction of a mixture of ammonium thiocyanate and 3-methoxybenzoyl chloride in dry acetone solvent, followed by a reflux reaction of 2,6-diaminopyridine with a yield of approximately 44% yield. Characterization using ^{1}H-NMR, ^{13}C-NMR, UV-Vis and FT-IR spectroscopy was performed on a pale-yellow aggregation and demonstrated that the reaction produced BT compound. The microwave irradiation synthesis was performed as alternative method to reflux heating method to give higher percentage yield (73.2 %) and reduce reaction time (from 24 h to 10 min). Interestingly, by using microwave irradiation method, aggregation and crystal were produced. X-ray crystallography was used to solve a crystal structure according to the actual structure of the compound. The comparison between the theoretical and experimental structure of the compound explained there is little difference in bond angles and bond length. While there is a difference in ligand geometry and coordinated with copper ions using the DFT method. The experimental results of copper binding with the BT compound were intriguing because the interaction of the ligand with the copper by thioamide and amide groups occurred via S and O atoms. The ligand structure's flexible rotation allowed it to easily trace the metal and bond quickly, resulting in a very fast color change. This could aid researchers in developing it as a future color sensor.

ACKNOWLEDGEMENTS

The authors gratefully acknowledge the Ministry of Higher Education, Malaysia under Fundamental Research Grant Scheme (FRGS) with the grant number of FRGS/1/2022/STG04/UKM/02/4) for funding this project. The authors would also like to thank the Centre for Research and Instrumentation Management (CRIM), UKM for providing facilities and Centre for Information and Communication Technology (CICT), Universiti Teknologi Malaysia (UTM) for high-performance computing to reduce the investigation time maintained (grant number FRGS/R.J130000.7854.5F471).

REFERENCES

Abosadiya, H.M., Anouar, E.H., Hasbullah, S.A. & Yamin, B.M. 2015. Synthesis, X-ray, NMR, FT-IR, UV/vis, DFT and TD-DFT studies of N-(4-chlorobutanoyl)-N′-(2-, 3- and 4-methylphenyl) thiourea derivatives. *Spectrochimica Acta - Part A: Molecular and Biomolecular Spectroscopy* 144: 115-124.

Adam, F., Fatihah, N.N. & Ameram, N. 2016. The synthesis and characterisation of 2-methyl-N- Its preparation with antibacterial study. *Journal of Physical Science* 27(2): 83-101.

Ajlouni, A.M., Taha, Z.A., Al-Hassan, K.A. & Abu Anzeh, A.M. 2012. Synthesis, characterization, luminescence properties and antioxidant activity of Ln(III) complexes with a new aryl amide bridging ligand. *Journal of Luminescence* 132(6): 1357-1363.

Alenzi, M.K., Azam, M., Al-Resayes, S.I., Kansız, S., Çamaş, A.S., Agurokpon, D.C., Louis, H., Kumar, V., Dege, N. & Alam, M. 2024. Experimental and theoretical investigation into the design of nickel (II), copper (II), and zinc (II) complexes substituted with pyrazole ligand. *Polyhedron* 259: 117073.

Al-Harbi, R.A.K., El-Sharief, M.A.M.S. & Abbas, S.Y. 2019. Synthesis and anticancer activity of bis-benzo[d] [1,3]dioxol-5-yl thiourea derivatives with molecular docking study. *Bioorganic Chemistry* 90: 103088.

Altaf, A.A., Shahzad, A., Gul, Z., Khan, S.A., Badshah, A., Tahir, M.N., Zafar, Z.I. & Khan, E. 2015. Synthesis, crystal structure, and DFT calculations of 1,3-diisobutyl thiourea. *Journal of Chemistry* 2015: 913435.

Antony Muthu Prabhu, A., Siva, S., Sankaranarayanan, R.K. & Rajendiran, N. 2010. Intramolecular proton transfer effects on 2,6-diaminopyridine. *Journal of Fluorescence* 20: 43-54.

Arshad, N., Shakeel, M., Javed, A., Perveen, F., Saeed, A., Ahmed, A., Ismail, H., Channar, P.A. & Naseer, F. 2024. Exploration of newly synthesized amantadine-thiourea conjugates for their DNA binding, anti-elastase, and anti-glioma potentials. *International Journal of Biological Macromolecules* 263(Part 1): 130231.

Arshad, N., Rafiq, M., Ujan, R., Saeed, A., Farooqi, S.I., Perveen, F., Channar, P.A., Ashraf, S., Abbas, Q., Ahmed, A., Hokelek, T., Kaur, M. & Jasinski, J.P. 2020. Synthesis, X-ray crystal structure elucidation and Hirshfeld surface analysis of N-((4-(1H-benzo[d] imidazole-2-yl)phenyl)carbamothioyl)benzamide: Investigations for elastase inhibition, antioxidant and DNA binding potentials for biological applications. *RSC Advances* 10: 20837-20851.

Baby, R., Saifullah, B. & Hussein, M.Z. 2019. Palm kernel shell as an effective adsorbent for the treatment of heavy metal contaminated water. *Scientific Reports* 9: 18955.

Bai, X., Li, Y. & Ye, Z. 2016. A colorimetric sensor based on thiourea–polyvinyl alcohol microspheres for the selective recognition of Hg^{2+} and Cu^{2+}. *New Journal of Chemistry* 40(10): 8815-8822.

Bruckmann, A., Krebs, A. & Bolm, C. 2008. Organocatalytic reactions: Effects of ball milling, microwave and ultrasound irradiation. *Green Chemistry* 10(11): 1131-1141.

Caprio, V. 2008. Pyridines and their benzo derivatives: Reactivity of substituents. *Comprehensive Heterocyclic Chemistry III* 5: 101-169.

Chacko Yohannan Panickera, H.T.V., Varkey, T., Georged, A. & Kandathil, P. 2010. FT-IR, FT-Raman and *ab-initio* studies of 1,3-diphenyl thiourea. *European Journal of Chemistry* 1(3): 173-178.

Charisiadis, P., Kontogianni, V.G., Tsiafoulis, C.G., Tzakos, A.G., Siskos, M. & Gerothanassis, I.P. 2014. 1H-NMR as a structural and analytical tool of intra- and intermolecular hydrogen bonds of phenol-containing natural products and model compounds. *Molecules* 19: 13643-13682.

Delgado, G.E., Fonseca, J.L., Mora, A.J., Bruno-Colmenárez, J., Chacón, C., Marroquin, G., Cisterna, J. & Brito, I. 2024. Crystal structure, hydrogen bond patterns, Hirshfeld surface analysis, and topological studies (NCI) of 1, 5, 5-trimethyl-imidazolidine-2, 4-dione; an organic compound with high symmetry crystallizing in the tetragonal space group *I*4/*m*. *Journal of Molecular Structure* 1299: 137205.

Dhanishta, P., Siva, P.S., Mishra, S.K. & Suryaprakash, N. 2018. Intramolecular hydrogen bond directed stable conformations of benzoyl phenyl oxalamides: Unambiguous evidence from extensive NMR studies and DFT-based computations. *RSC Advances* 8(20): 11230-11240.

Dudley, G.B. & Stiegman, A.E. 2015. On the existence of and mechanism for microwave-specific reaction rate enhancement. *Chemical Science* 6: 2144-2152.

Effendhy, N.D., Roto, R. & Siswanta, D. 2024. Advancing fluoride (F–) detection: Exploring the potential of digital color analysis with a novel thiourea receptor. *Microchemical Journal* 197: 109819.

Fakhar, I., Yamin, B.M. & Hasbullah, S.A. 2017. A comparative study of the metal binding behavior of alanine based bis-thiourea isomers. *Chemistry Central Journal* 11: 76.

Fakhar, I., Yamin, B.M. & Hasbullah, S.A. 2016. Synthesis and characterization of bis-thiourea having amino acid derivatives. *AIP Conference Proceedings* 1784: 030012.

Gemili, M., Nural, Y., Keleş, E., Aydıner, B., Seferoğlu, N., Sahin, E., Sarı, H. & Seferoğlu, Z. 2018. Novel 1,4-naphthoquinone N-aroylthioureas: Syntheses, crystal structure, anion recognition properties, DFT studies and determination of acid dissociation constants. *Journal of Molecular Liquids* 269: 920-932.

Han, W.S., Lee, H.Y., Jung, S.H. & Lee, S.J. 2009. Silica-based chromogenic and fluorogenic hybrid chemosensor materials. *Chemical Society Reviews* 38(7): 1904-1915.

Hosseinjani-Pirdehi, H., Mahmoodi, N.O., Pasandideh, M. & Taheri, A. 2020. Novel synthesized azo-benzylidene-thiourea as dual naked-eye chemosensor for selective detection of Hg^{2+} and CN^{-} ions. *Journal of Photochemistry & Photobiology A: Chemistry* 391: 112365.

Imran Fakhar, Bohari Muhammad Yamin, Sahilah Abdul Mutalib & Siti Aishah Hasbullah. 2018. Synthesis and binding behaviour of new isomers of bis-thiourea. *Sains Malaysiana* 47(6): 1199-1208.

Jambi, S.M., Chen, J., Zhang, W., Fu, S., Zhou, Y., Domena, J.B. & Leblanc, R.M. 2023. Synthesis and characterization of carbon dots derived from compounds containing thioureas and thiazole rings. *Colloids and Surfaces A: Physicochemical and Engineering Aspects* 669: 131522.

Jin, G., Hong, I., Joo, E., Kim, H. & Kim, C. 2014. A colorimetric and fluorescent sensor for sequential detection of copper ion and cyanide. *Tetrahedron* 70(17): 2822-2828. http://dx.doi.org/10.1016/j.tet.2014.02.055

Jorgetto, A.D.O., Pereira, S.P., Innocenti, R., Saeki, M.J., Antonio, M., Martines, U., Pedrosa, V.D.A. & Castro, G.R. 2015. Application of mesoporous SBA-15 silica functionalized with 4-amino-2-mercaptopyrimidine for the adsorption of Cu(II), Zn(II), Cd(II), Ni(II), and Pb(II) from water. *Acta Chimica Slovenica* 62(1): 111-121.

Kamalulazmy, N., Mutalib, S.A., Nasir, F.I. & Hassan, N.I. 2016. Characterization and antimicrobial studies of five substituted bis-thioureas. *Malaysian Journal of Analytical Sciences* 20(1): 85-90.

Klygach, D.S., Vakhitov, M.G., Suvorov, P.V., Zherebtsov, D.A. & Trukhanov, S.V. 2019. Magnetic and microwave properties of carbonyl iron in the high frequency range. *Journal of Magnetism and Magnetic Materials* 490: 165493.

Kole, G.K. & Kumar, M. 2018. Patterns of hydrogen bonding involving thiourea in the series of thiourea·trans-1,2-bispyridyl ethylene cocrystals–A comparative study. *Journal of Molecular Structure* 1163: 18-21.

Lin, Q., Chen, P., Liu, J., Fu, Y., Zhang, Y. & Wei, T. 2013. Colorimetric chemosensor and test kit for detection copper (II) cations in aqueous solution with specific selectivity and high sensitivity. *Dyes and Pigments* 98(1): 100-105. http://dx.doi.org/10.1016/j.dyepig.2013.01.024

Liu, Y., Yang, L., Li, L., Liang, X., Li, S. & Fu, Y. 2020. A dual thiourea-appended perylenebisimide "turn-on" fluorescent chemosensor with high selectivity and sensitivity for Hg^{2+} in living cells. *Spectrochimica Acta Part A: Molecular and Biomolecular Spectroscopy* 241: 118678.

Lu, A., Wang, Z., Zhou, Z., Chen, J. & Wang, Q. 2015. Application of "hydrogen bonding interaction" in new drug development : Design, synthesis, antiviral activity and SARs of thiourea derivatives. *Journal of Agricultural and Food Chemistry* 63(5): 1378-1384.

Luo, J., Hunyar, C., Feher, L., Link, G., Thumm, M. & Pozzo, P. 2004. Theory and experiments of electromagnetic loss mechanism for microwave heating of powdered metals. *Applied Physics Letters* 84(25): 5076-5078.

Maddani, M.R. & Prabhu, K.R. 2010. A concise synthesis of substituted thiourea derivatives in aqueous medium. *The Journal of Organic Chemistry* 75(7): 2327-2332.

Maity, D. & Govindaraju, T. 2011. Highly selective visible and near-IR sensing of Cu^{2+} based on thiourea–Salicylaldehyde coordination in aqueous media. *Chemistry - A European Journal* 17(5): 1410-1414.

Mohd, W., Wan, K., Zin, M., Kadir, M.A. & Yamin, B.M. 2011. Structural and spectroscopic studies of novel methylbenzoyl thiourea derivatives. *Malaysian Journal of Analytical Sciences* 15(1): 70-80.

Ngah, F.A.A., Zakariah, E.I., Hassan, N.I., Yamin, B., Sapari, S. & Hasbullah, S.A. 2017. Synthesis of thiourea derivatives and binding behavior towards the mercury ion. *Malaysian Journal of Analytical Sciences* 21(6): 1226-1234.

Nurul Hidayah Abdul Razak, Ling Ling Tan, Siti Aishah Hasbullah & Lee Yook Heng. 2020. Reflectance chemosensor based on bis-thiourea derivative as ionophore for copper(II) ion detection. *Microchemical Journal* 153: 104460.

Perrone, D., Monteiro, M. & Castelo-Branco, V.N. 2015. The chemistry of imidazole dipeptides. In *Imidazole Dipeptides: Chemistry, Analysis, Function and Effects,* edited by Preedy, V.R. Cambridge: Royal Society of Chemistry. pp. 43-60.

Pingaew, R., Sinthupoom, N., Mandi, P., Prachayasittikul, V., Cherdtrakulkiat, R., Prachayasittikul, S., Ruchirawat, S. & Prachayasittikul, V. 2017. Synthesis, biological evaluation and *in silico* study of bis-thiourea derivatives as anticancer, antimalarial and antimicrobial agents. *Medicinal Chemistry Research* 26(12): 3136-3148.

Reisman, S.E., Doyle, A.G. & Jacobsen, E.N. 2008. Enantioselective thiourea-catalyzed additions to oxocarbenium ions. *Journal of the American Chemical Society* 130(23): 7198-7199.

Robinson, J., Kingman, S., Irvine, D., Licence, P., Smith, A., Dimitrakis, G. & Kappe, C.O. 2010. Understanding microwave heating effects in single mode type cavities-theory and experiment. *Physical Chemistry Chemical Physics* 12: 4750-4758.

Saad, F.A. 2014. Synthesis, spectral, electrochemical and X-ray single crystal studies on Ni(II) and Co(II) complexes derived from 1-benzoyl-3-(4-methylpyridin-2-yl) thiourea. *Spectrochimica Acta Part A: Molecular and Biomolecular Spectroscopy* 128: 386-392.

Sapari, S., Emma Izzati Zakariah, Razak, N.H.A., Ramzan, I., Numin, M.S., Lee Yook Heng & Hasbullah, S.A. 2021. A comparative study of microwave-assisted and conventional heating methods of the synthesis of 1-(naphthalene-1-yl)-3-(o, m, p-tolyl)thioureas, dft analysis, antibacterial evaluation and drug-likeness assessment. *Sains Malaysiana* 50(3): 743-751.

Schroeder, D.C. 1955. Thioureas. *Chemical Reviews* 55(1): 181-228.

Tang, J., Radosz, M. & Shen, Y. 2008. Poly (ionic liquid) s as optically transparent microwave-absorbing materials. *Macromolecules* 41: 493-496.

Teixeira, A.M.R., Santos, H.S., Albuquerque, M.R.J.R., Bandeira, P.N., Rodrigues, A.S., Silva, C.B., Gusmão, G.O.M., Freire, P.T.C. & Bento, R.R.F. 2012. Vibrational spectroscopy of xanthoxyline crystals and DFT calculations. *Brazilian Journal of Physics* 42(3-4): 180-185.

Tungsombatvisit, N., Inprasit, T., Rohmawati, D. & Pisitsak, P. 2019. Rhodamine derivative- based cellulose acetate electrospun colorimetric sensor for Cu^{2+} sensing in water: Effects of alkaline treatment. *Fibers and Polymers* 20(3): 481-489.

Warren, W.H. 1928. Contemporary reception of Wohler's discovery of the synthesis of urea. *Journal of Chemical Education* 5(12): 1539.

Wazzan, N.A. 2015. DFT calculations of thiosemicarbazide, arylisothiocynates, and 1-aryl-2,5-dithiohydrazodicarbonamides as corrosion inhibitors of copper in an aqueous chloride solution. *Journal of Industrial and Engineering Chemistry* 26: 291-308.

Wiberg, K.B., Wang, Y., Box, P.O. & Haven, N. 2011. A comparison of some properties of C=O and C=S bonds. *Arkivoc* 2011(5): 45-56.

Yang, Y., Weaver, M.N. & Merz Jr., K.M. 2009. Assessment of the "6-31+G** + LANL2DZ" Mixed basis set coupled with density functional theory methods and the effective core potential : Prediction of heats of formation and ionization potentials for first-row-transition-metal complexes. *Journal of Physical Chemistry A* 113(36): 9843-9851.

*Corresponding author; email: aishah80@ukm.edu.my